1 Supplementary Material

Figure S1: Relative Humidity (%) for Time-Mean - TM [**(a)**, **(c)**, **(e)**, **(g)**] and Standard Deviation - SD [**(b)**, **(d)**, **(f)**, **(h)**] from 1980-2005. The first row for the JRA55 reanalysis; the second row for the difference between ensemble average of CMIP5 (raw) and JRA-55; and the subsequent rows for the difference between corrected CMIP5 and JRA-55 with BC methods used (linear scaling - LS and quantile mapping - QM, respectively).

(a) JRA-55 TM

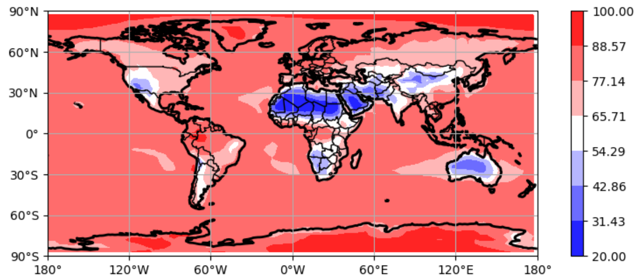

(b) JRA-55 SD

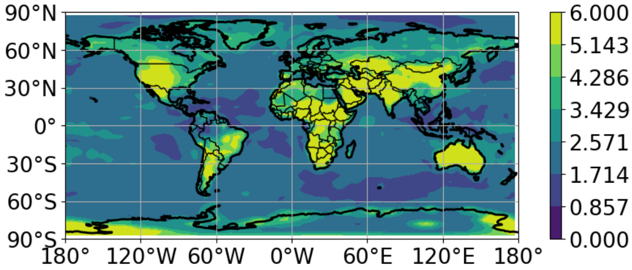

(c) CMIP5-JRA-55 TM

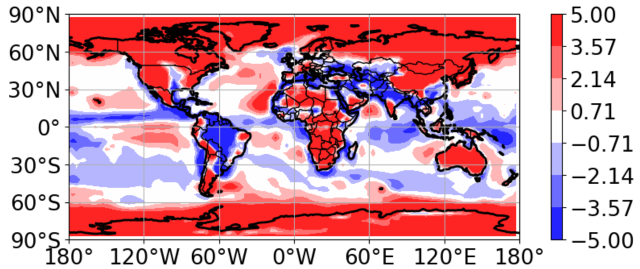

(d) CMIP5-JRA-55 SD

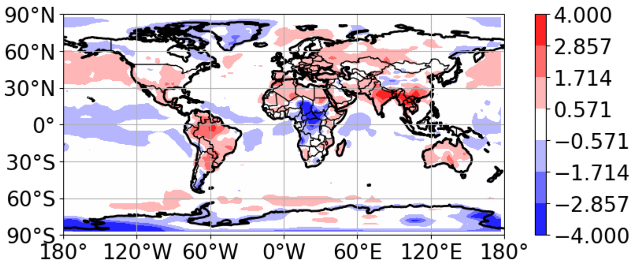

(e) CMIP5 LS-JRA-55 TM

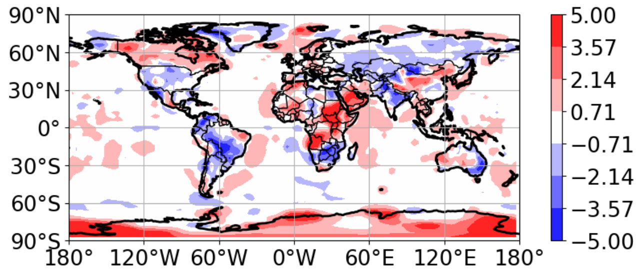

(f) CMIP5 LS-JRA-55 SD

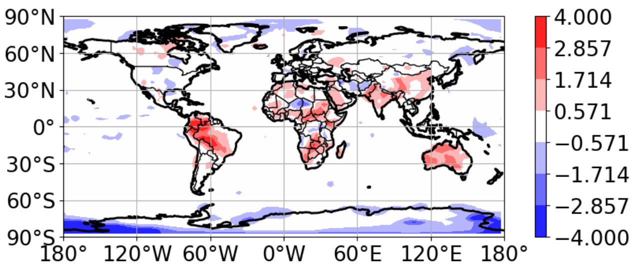

(g) CMIP5 QM-JRA-55 TM

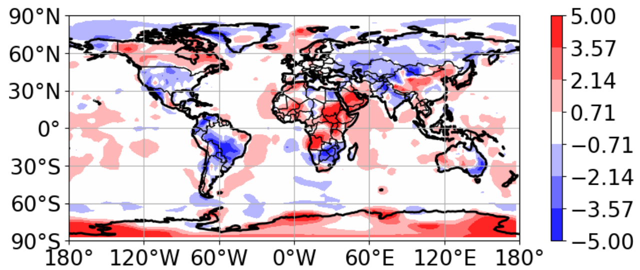

(h) CMIP5 QM-JRA-55 SD

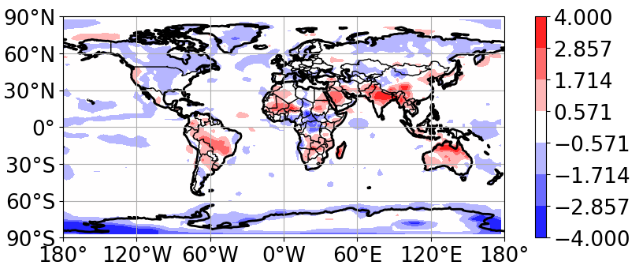

Figure S2: Sea level pressure (Pa) for Time-Mean - TM [**(a), (c), (e), (g)**] and Standard Deviation - SD [**(b), (d), (f), (h)**] from 1980-2005. The first row for the JRA55 reanalysis; the second row for the difference between ensemble average of CMIP5 (raw) and JRA-55; and the subsequent rows for the difference between corrected CMIP5 and JRA-55 with BC methods used (linear scaling - LS and quantile mapping - QM, respectively).

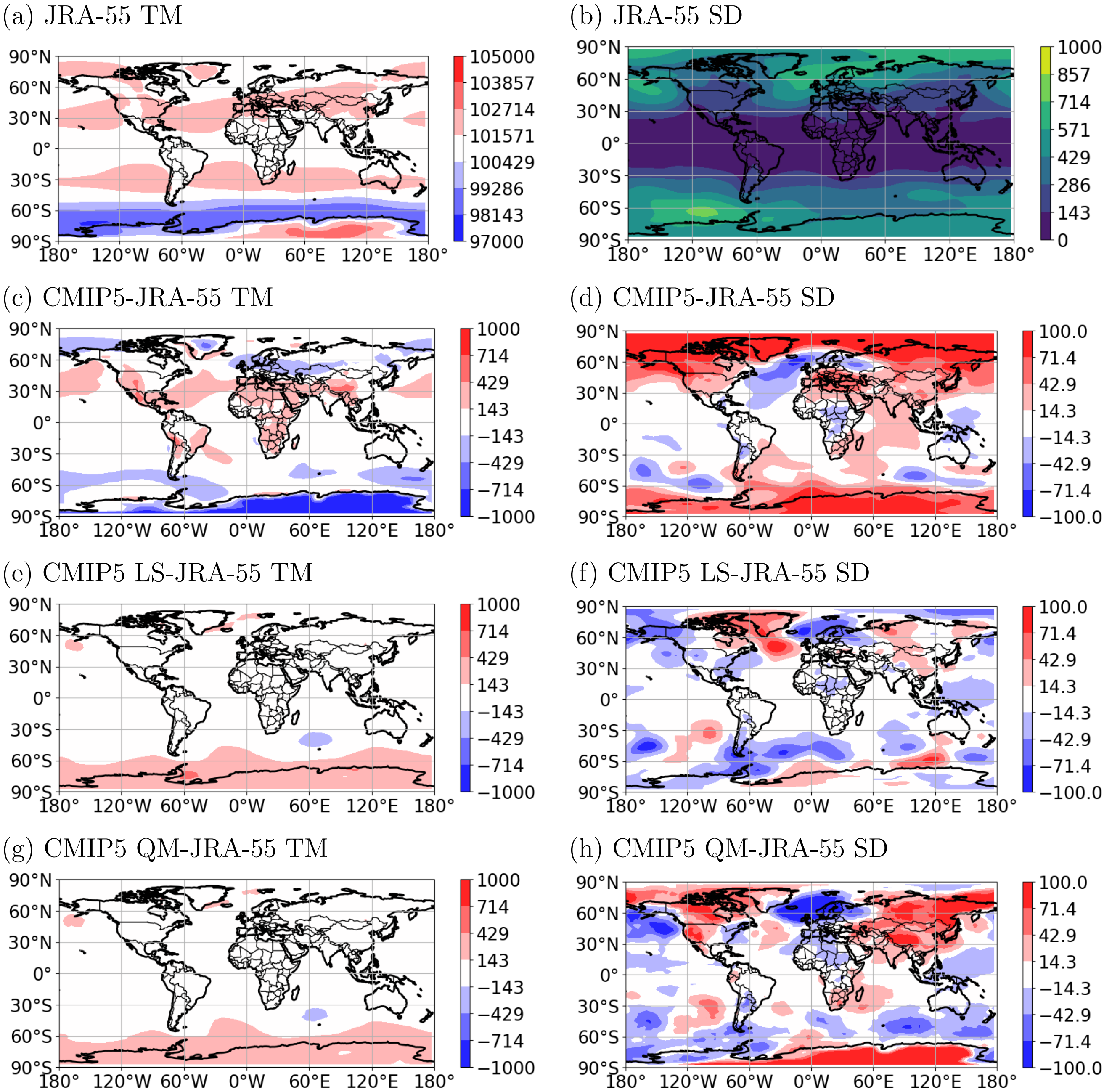

Figure S3: Taylor diagrams showing the performance of the GCMs and BC methods. The translucent dots are the individual models, and the solid ones are for the ensemble mean. For relative humidity: **(a)** mean; **(b)** standard deviation. For sea level pressure: **(c)** mean; **(d)** standard deviation.

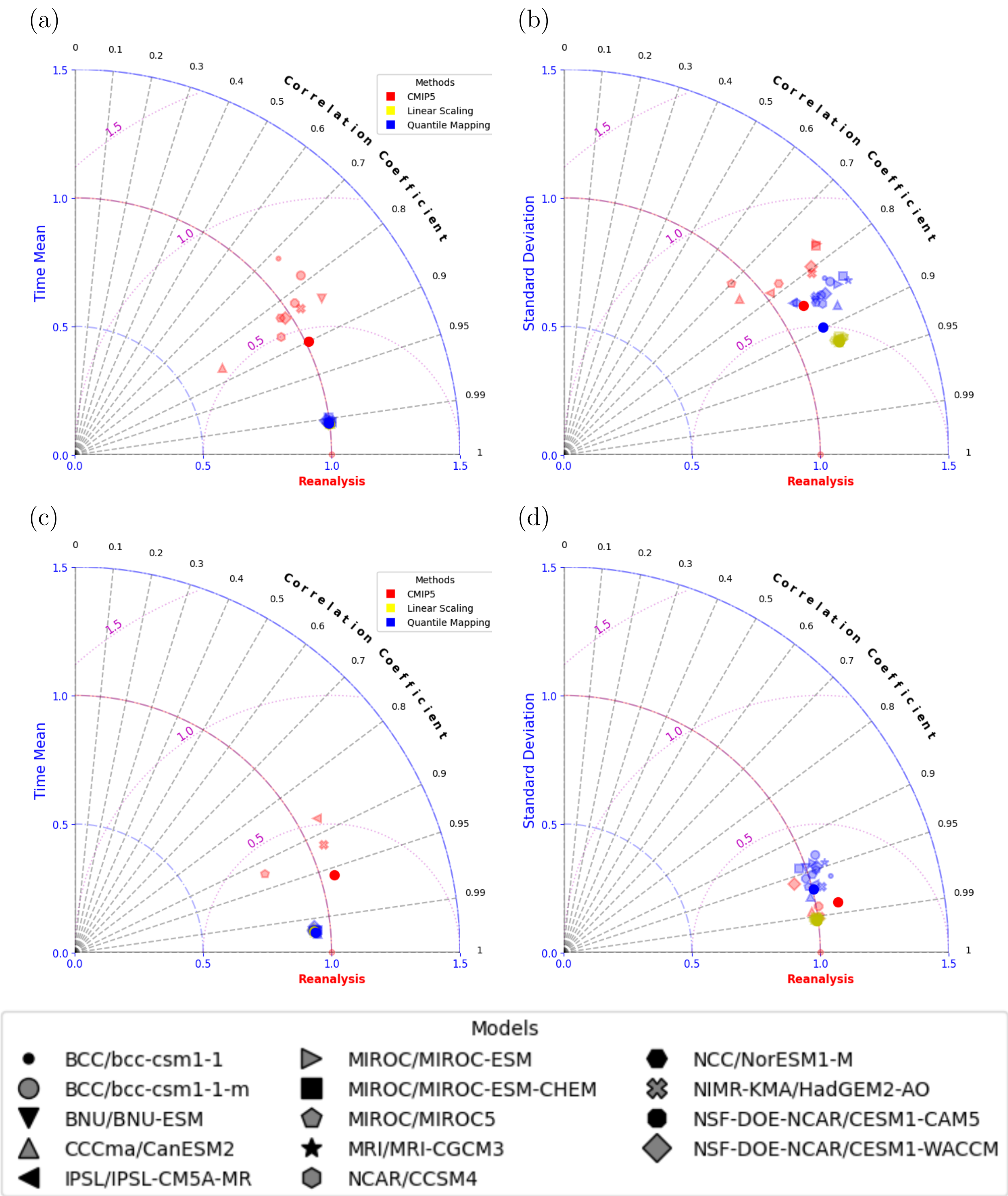

Figure S4: Boxplots of relative humidity (%) future projections (RCP2.6, RCP4.5, and RCP8.5 scenarios) for the time-mean [**(a), (c), (e)**] and standard deviation [**(b), (d), (f)**] considering raw CMIP5 and the two BC methods used (linear scaling and quantile mapping). Each boxplot represents the distribution across CMIP5 models, where each value corresponds to one model after spatial averaging over the respective region. The secondary vertical axis on the right-hand side of each plot represents the increase in values relative to the reanalysis. The central line indicates the median, the box bounds the interquartile range - IQR (25th–75th percentiles), and whiskers extend to 1.5x the IQR. The first row corresponds to the global scale, the second to Brazil, and the third to the state of Minas Gerais.

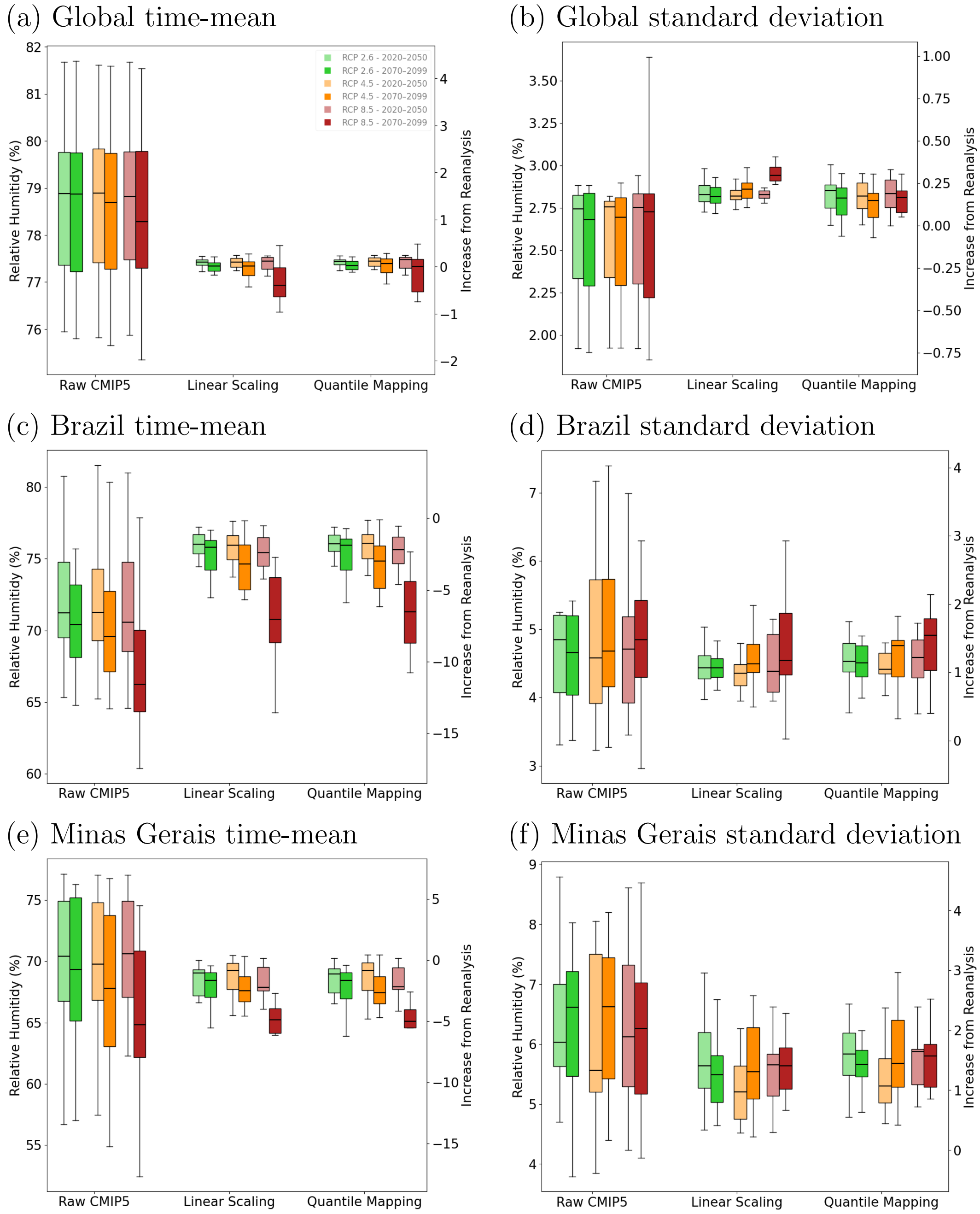

Figure S5: Boxplots of sea-level pressure (Pa) future projections (RCP2.6, RCP4.5, and RCP8.5 scenarios) for the time-mean [**(a), (c), (e)**] and standard deviation [**(b), (d), (f)**] considering raw CMIP5 and the two BC methods used (linear scaling and quantile mapping). Each boxplot represents the distribution across CMIP5 models, where each value corresponds to one model after spatial averaging over the respective region. The secondary vertical axis on the right-hand side of each plot represents the increase in values relative to the reanalysis. The central line indicates the median, the box bounds the interquartile range - IQR (25th–75th percentiles), and whiskers extend to 1.5x the IQR. The first row corresponds to the global scale, the second to Brazil, and the third to the state of Minas Gerais.

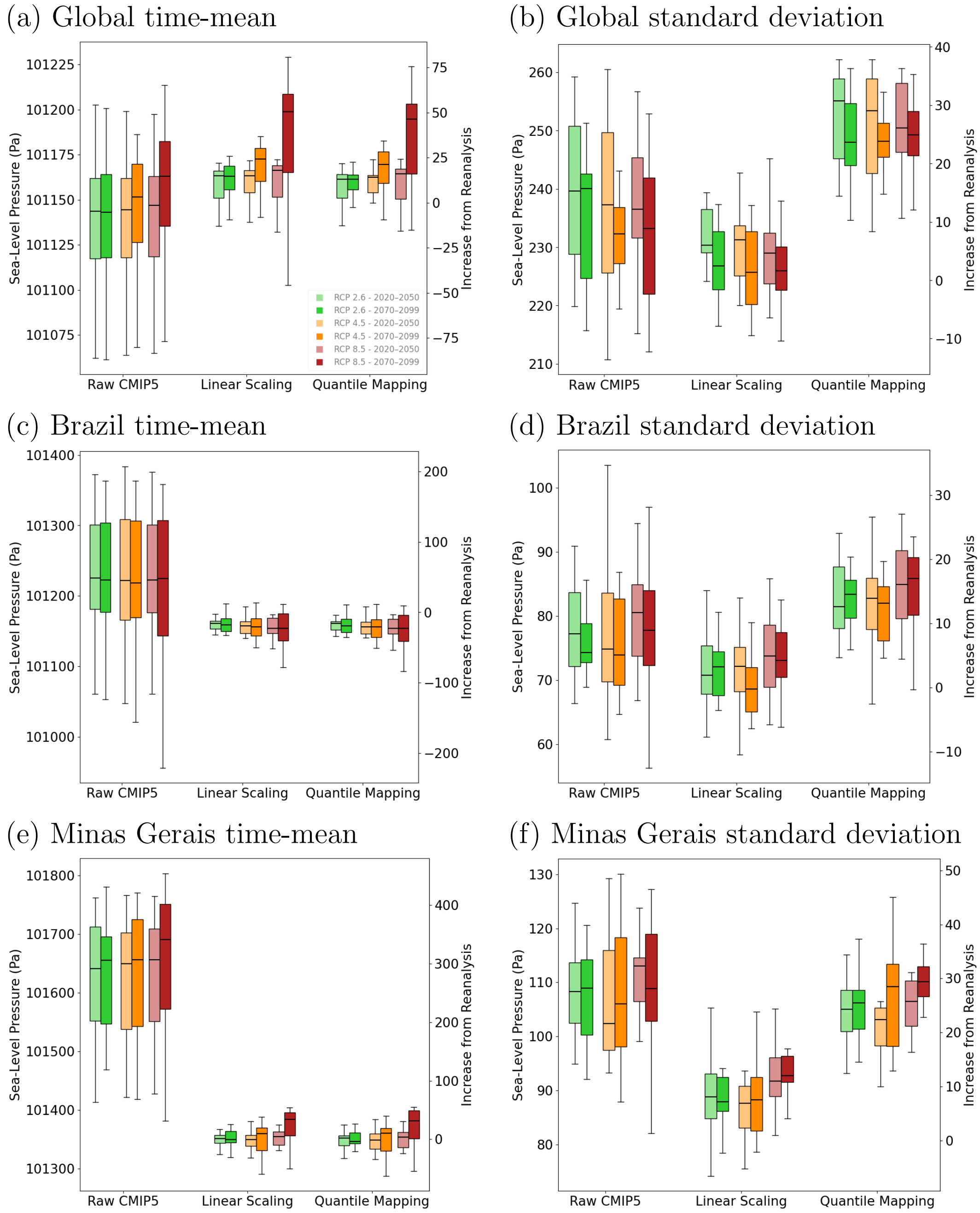

Figure S6: QuickClim relative humidity (%) - RH [**(a)**, **(c)**, **(e)**] and sea-level pressure (Pa) - SLP [**(b)**, **(d)**, **(f)**] projections with selected BC methods and raw CMIP5 at different spatial scales. The median values are represented by the solid lines and the shaded regions indicate the 25th and 75th percentiles. The first row for global average scale; the second row for the continental scale (Brazil average); and the third row for the local scale (Brazilian state of Minas Gerais average).

(a) Global RH time-mean

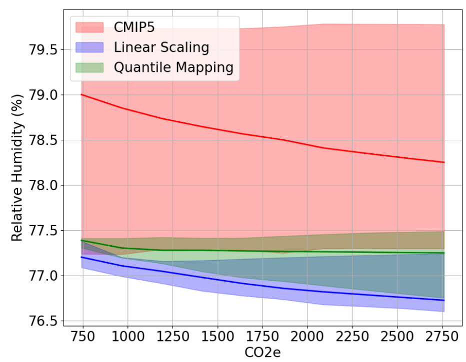

(b) Global SLP time-mean

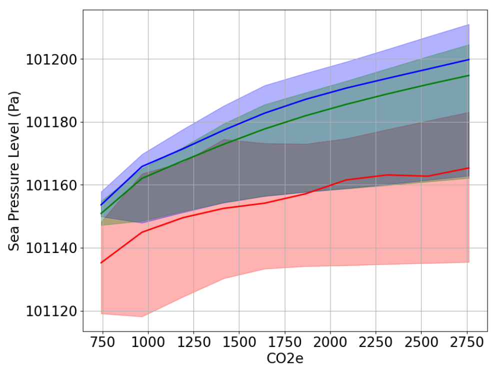

(c) Brazil RH time-mean

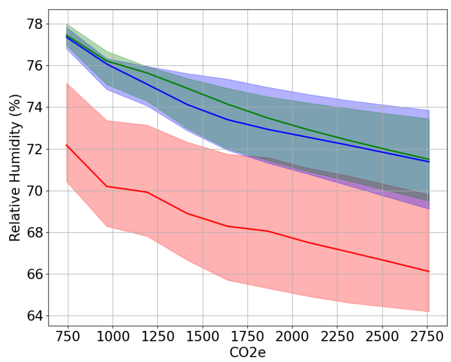

(d) Brazil SLP time-mean

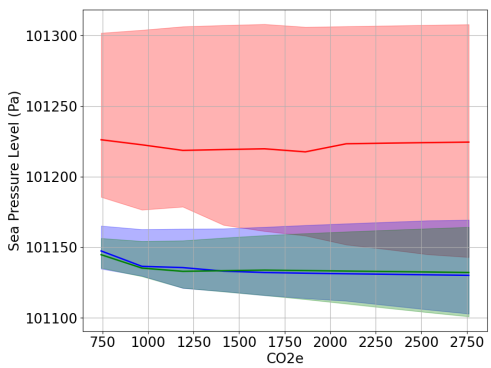

(e) Minas Gerais RH time-mean

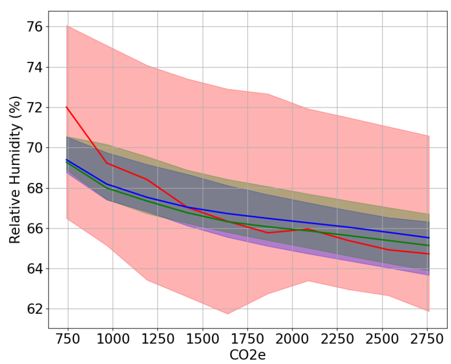

(f) Minas Gerais SLP time-mean

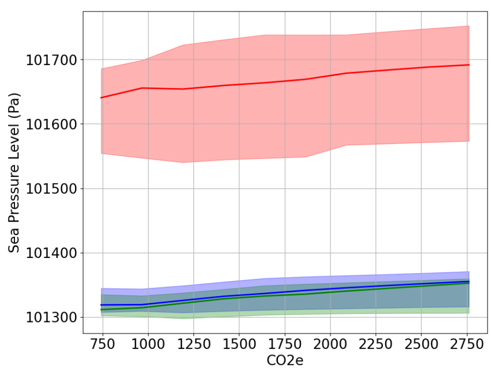

Figure S7: Spatial distribution of the mean differences between CMIP5 simulations and the JRA-55 reference dataset for relavite humidity - RH [**(a), (c), (e)**] and sea-level pressure - SPL [**(b), (d), (f)**]. The colors indicate the magnitude and sign of the mean differences, and the stippled areas represent regions where the differences are statistically significant at the 5% level ($p < 0.05$).

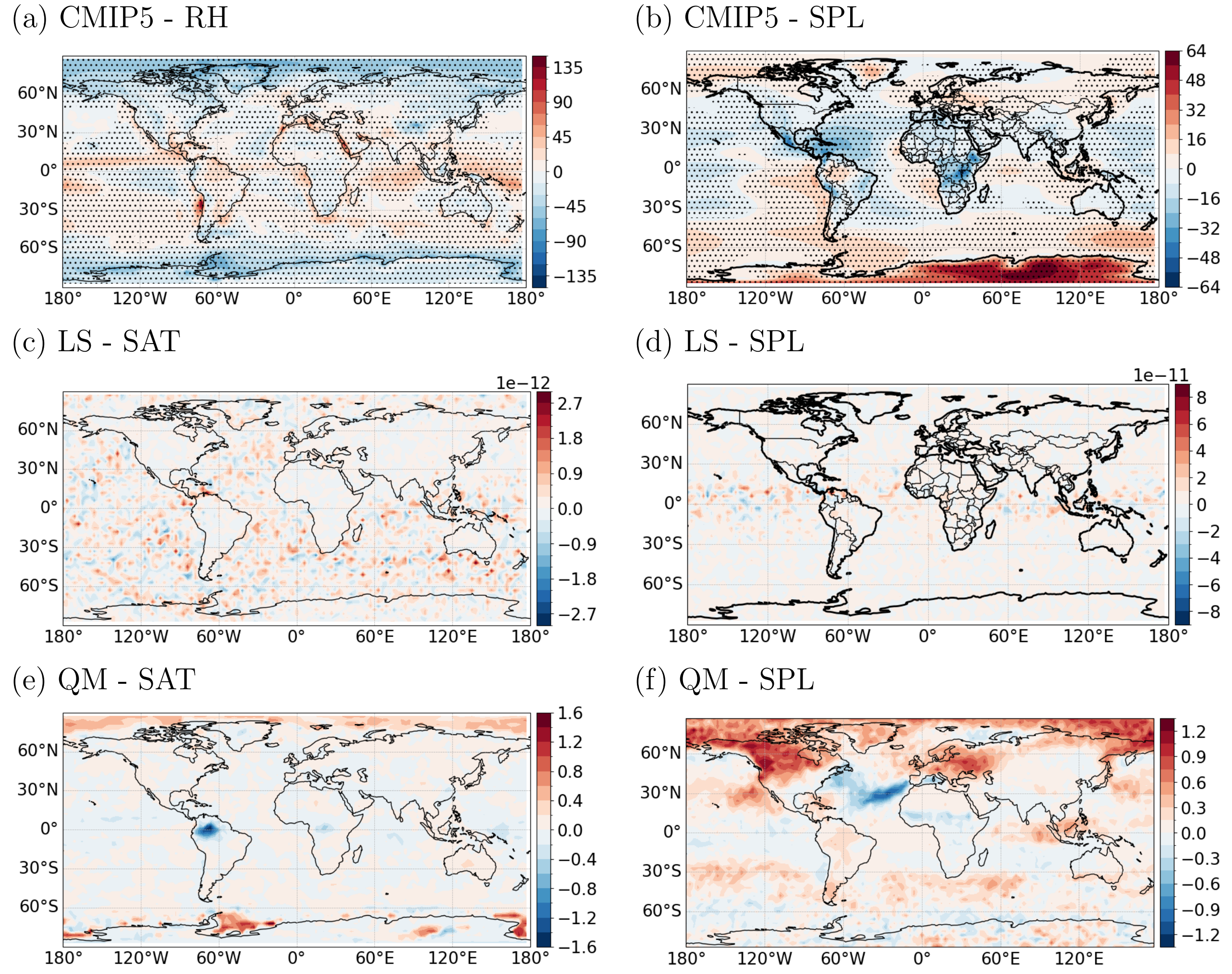

Figure S8: Uncertainty decomposition of global relative humidity projections. Fractional uncertainty (90% confidence interval) for (a) raw CMIP5, (b) linear scaling, and (c) quantile mapping and the corresponding proportion of variance attributed to internal variability (I), model uncertainty (M), and scenario uncertainty (S).

(a) Raw CMIP5 uncertainty decomposition.

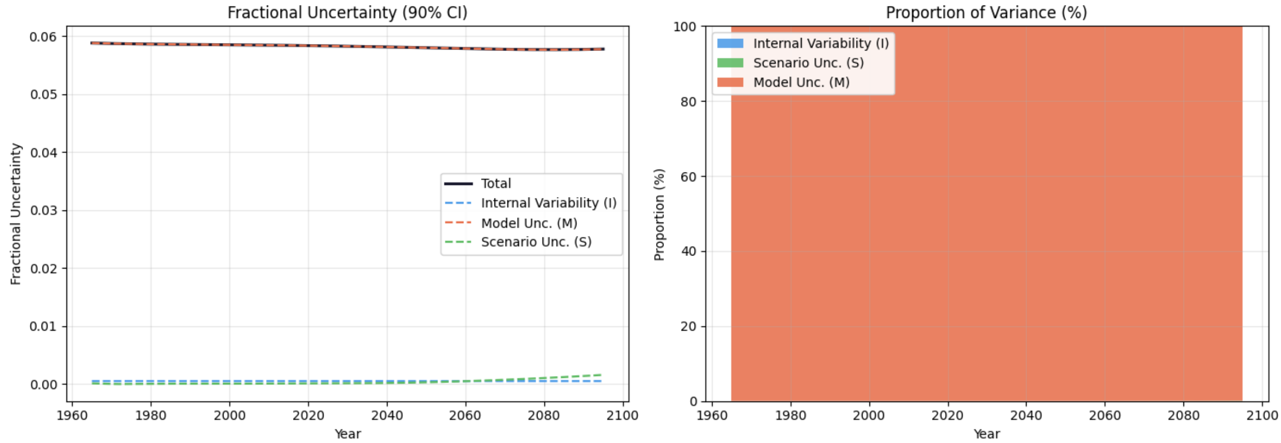

(b) Linear scaling uncertainty decomposition.

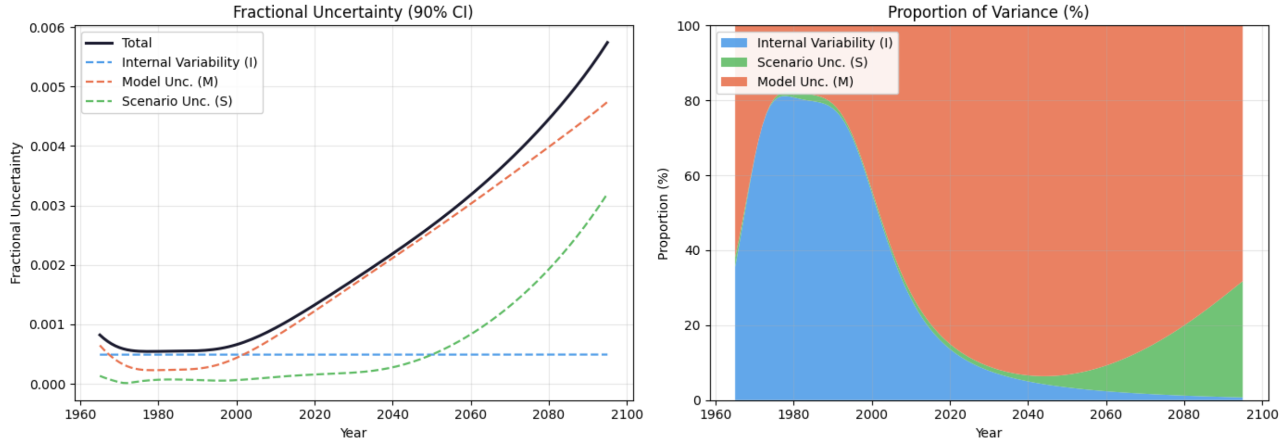

(c) Quantile mapping uncertainty decomposition.

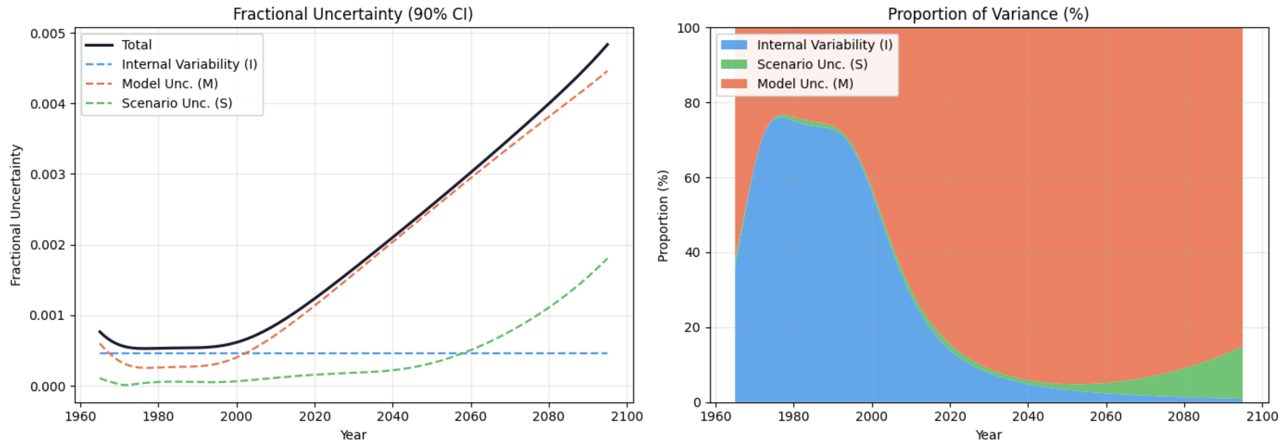

Figure S9: Uncertainty decomposition of global sea-level pressure projections. Fractional uncertainty (90% confidence interval) for (a) raw CMIP5, (b) linear scaling, and (c) quantile mapping and the corresponding proportion of variance attributed to internal variability (I), model uncertainty (M), and scenario uncertainty (S).

(a) Raw CMIP5 uncertainty decomposition.

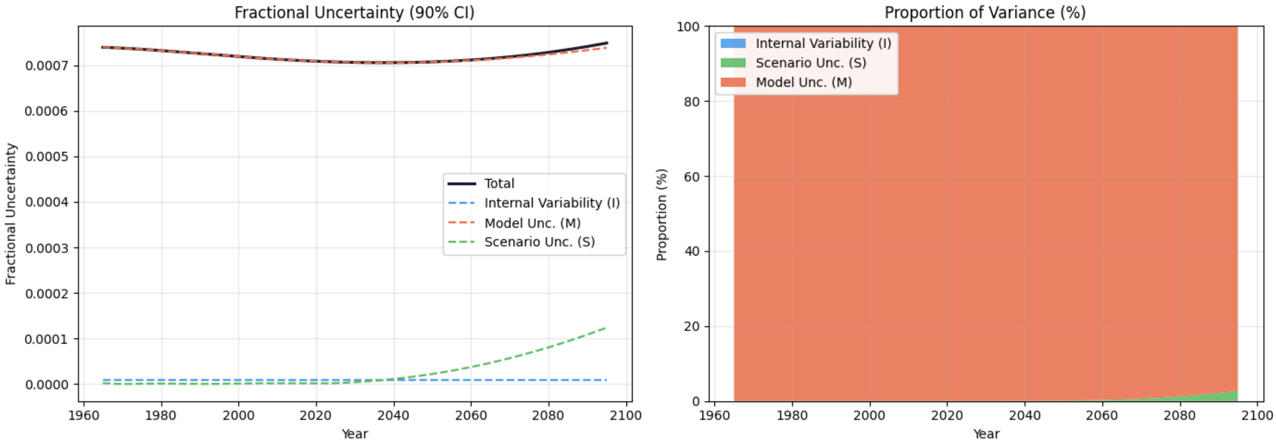

(b) Linear scaling uncertainty decomposition.

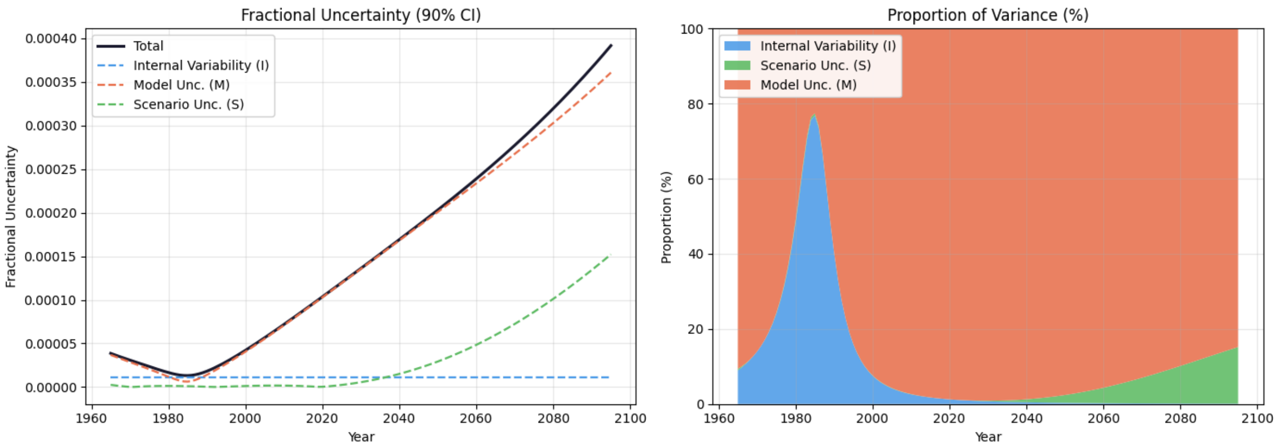

(c) Quantile mapping uncertainty decomposition.

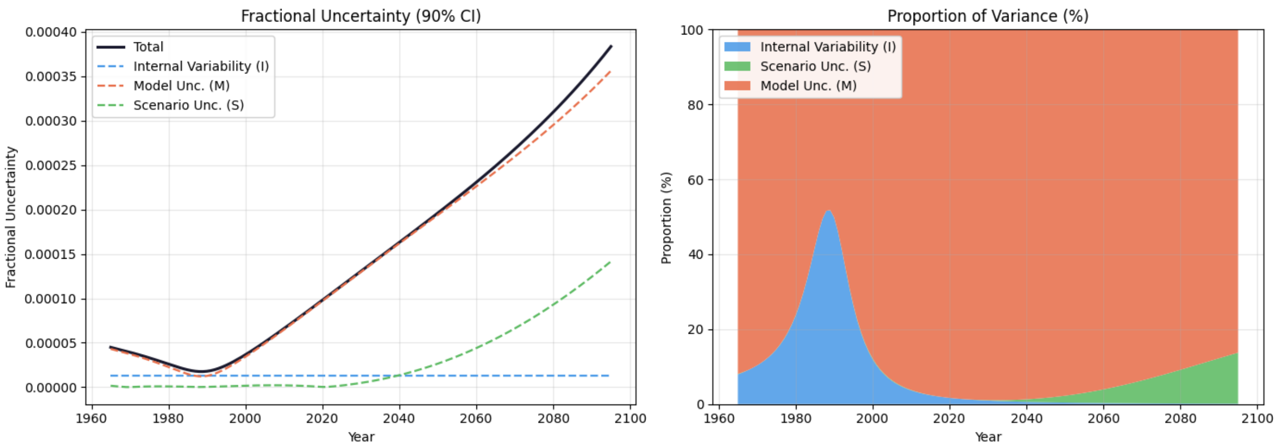

Figure S10: Uncertainty decomposition of Quickclim-derived WBGT projections. Fractional uncertainty (90% confidence interval) for (a) raw CMIP5, (b) linear scaling, and (c) quantile mapping and the corresponding proportion of variance attributed to internal variability (I), model uncertainty (M), and scenario uncertainty (S).

(a) Raw CMIP5 uncertainty decomposition.

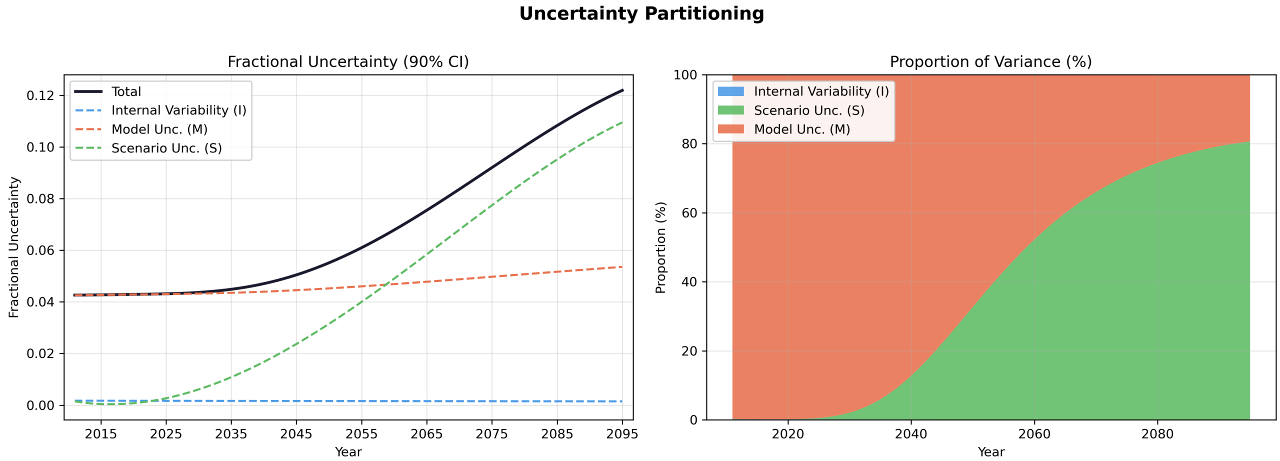

(b) Linear scaling uncertainty decomposition.

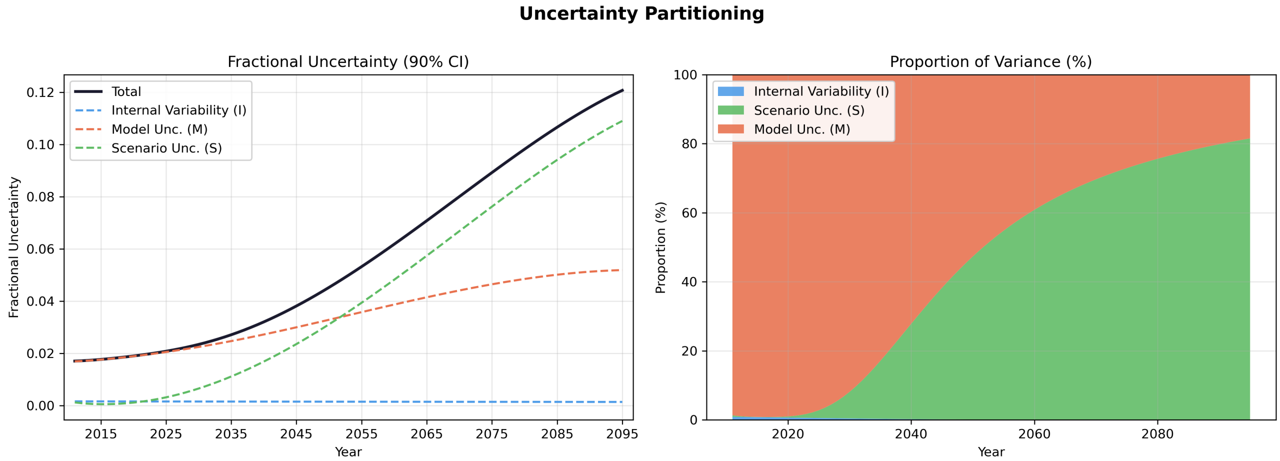

(c) Quantile mapping uncertainty decomposition.

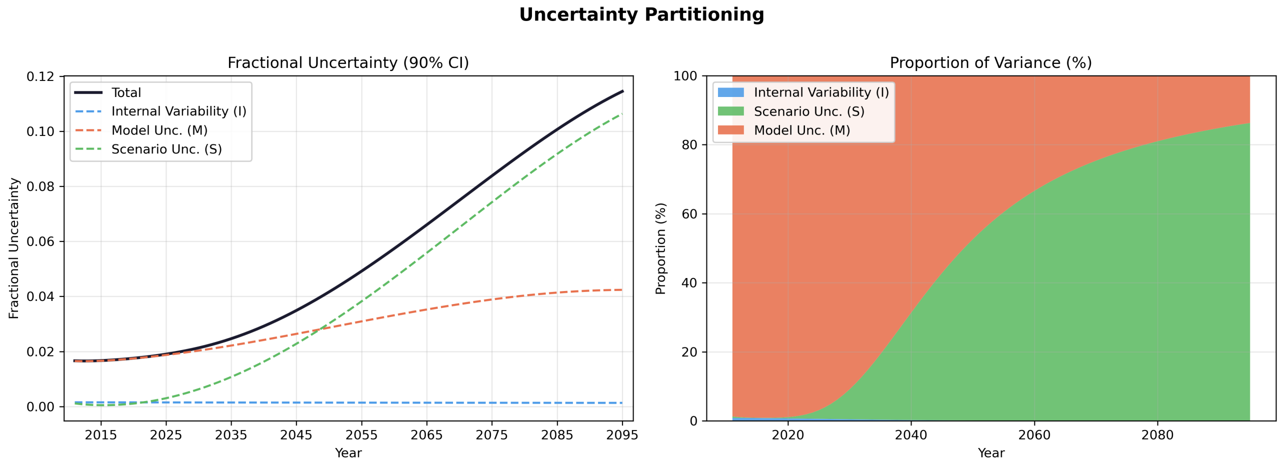

Figure S11: Uncertainty decomposition of Quickclim-derived labour productivity projections. Fractional uncertainty (90% confidence interval) for (a) raw CMIP5, (b) linear scaling, and (c) quantile mapping and the corresponding proportion of variance attributed to internal variability (I), model uncertainty (M), and scenario uncertainty (S).

(a) Raw CMIP5 uncertainty decomposition.

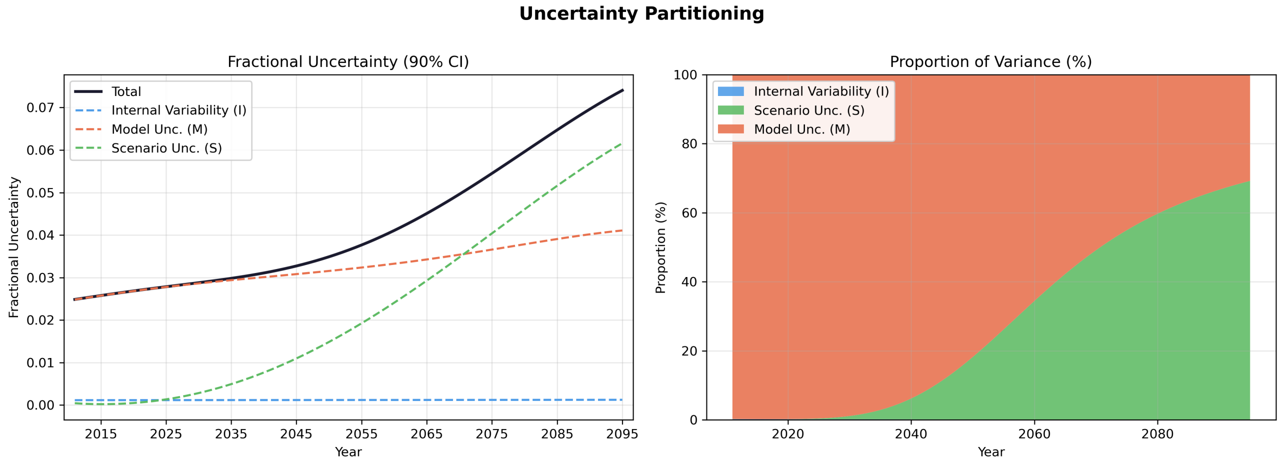

(b) Linear scaling uncertainty decomposition.

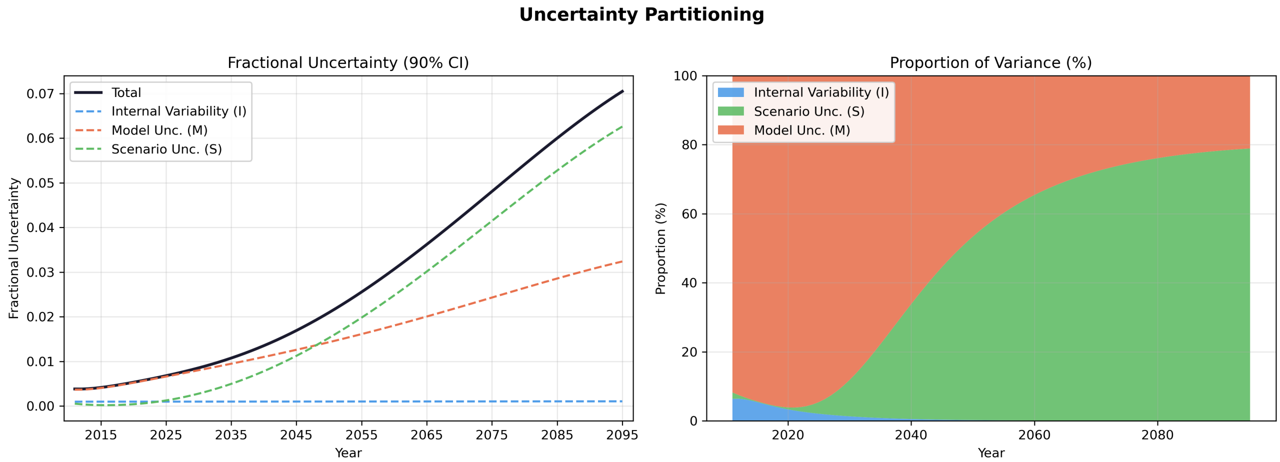

(c) Quantile mapping uncertainty decomposition.

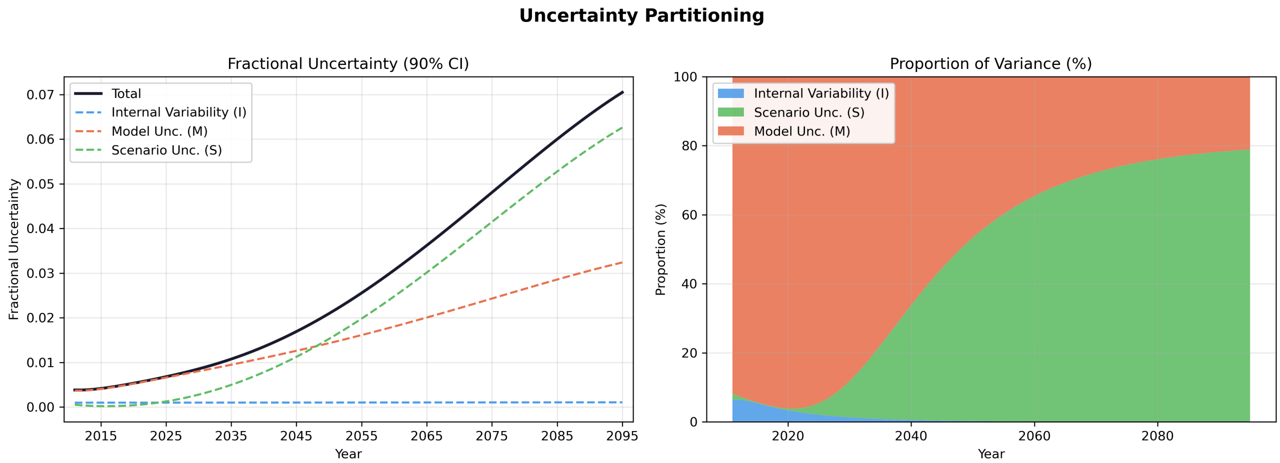

Table B1: CMIP5 models used in this study. In bold are highlighted only the GCMs that provide the necessary data.

Models	**Organization**
BCC/bcc-csm1-1 **BCC/bcc-csm1-1-m**	Beijing Climate Center, China Meteorological Administration
BNU/BNU-ESM	The Beijing Normal University
CCCma/CanESM2	Canadian Centre for Climate Modelling and Analysis
CMCC/CMCC-CESM CMCC/CMCC-CM CMCC/CMCC-CMS	Centro Euro-Mediterraneo per I Cambiamenti Climatici
CNRM-CERFACS/CNRM-CM5-2	Centre National de Recherches Meteorologiques/ Centre Europeen de Recherche et Formation Avancees en Calcul Scientifique
CSIRO-BOM/ACCESS1-0 CSIRO-BOM/ACCESS1-3	Commonwealth Scientific and Industrial Research Organisation (CSIRO) and Bureau of Meteorology (BOM)
FIO/FIO-ESM	First Institute of Oceanography
INM/inmcm4	Institute for Numeral Mathematics
IPSL/IPSL-CM5A-LR **IPSL/IPSL-CM5A-MR** IPSL/IPSL-CM5B-LR	Institut Pierre-Simon Laplace
LASG-CESS/FGOALS-g2	LASG, Institute of Atmospheric Physics, Chinese Academy of Sciences; and CESS, Tsinghua University
MIROC/MIROC-ESM **MIROC/MIROC-ESM-CHEM** MIROC/MIROC4h **MIROC/MIROC5**	Atmosphere and Ocean Research Institute (The University of Tokyo), National Institute for Environmental Studies, and Japan Agency for Marine-Earth Science and Technology
MOHC/HadGEM2-CC MOHC/HadGEM2-ES	Met Office Hadley Centre
MPI-M/MPI-ESM-LR MPI-M/MPI-ESM-MR MPI-M/MPI-ESM-P	Max Planck Institute for Meteorology
MRI/MRI-CGCM3 MRI/MRI-ESM1	Meteorological Research Institute
NASA-GISS/GISS-E2-H NASA-GISS/GISS-E2-H-CC NASA-GISS/GISS-E2-R NASA-GISS/GISS-E2-R-CC	NASA's Goddard Institute for Space Studies
NCAR/CCSM4	National Center for Atmospheric Research
NCC/NorESM1-M NCC/NorESM1-ME	Norwegian Climate Centre
NIMR-KMA/HadGEM2-AO	National Institute of Meteorological Research/ Korea Meteorological Administration
NOAA-GFDL/GFDL-CM3 NOAA-GFDL/GFDL-ESM2G NOAA-GFDL/GFDL-ESM2M	Geophysical Fluid Dynamics Laboratory
NSF-DOE-NCAR/CESM1-BGC **NSF-DOE-NCAR/CESM1-CAM5** NSF-DOE-NCAR/CESM1-FASTCHEM **NSF-DOE-NCAR/CESM1-WACCM**	National Science Foundation, Department of Energy, National Center for Atmospheric Research